Plasma measurements in the Jovian polar region with Juno/JADE

J. R. Szalay, F. Allegrini, F. Bagenal, S. Bolton, G. Clark, J. E. P. Connerney, L. P. Dougherty, R. W. Ebert, D. J. Gershman, W. S. Kurth, et al.

AGU PUBLICATIONS

Geophysical Research Letters

RESEARCH LETTER
10.1002/2017GL072837

Special Section:
Early Results: Juno at Jupiter

Plasma measurements in the Jovian polar region with Juno/JADE

J. R. Szalay[1], F. Allegrini[1,2], F. Bagenal[3], S. Bolton[1], G. Clark[4], J. E. P. Connerney[5], L. P. Dougherty[3], R. W. Ebert[1], D. J. Gershman[5], W. S. Kurth[6], S. Levin[7], P. Louarn[8], B. Mauk[4], D. J. McComas[1,9,10], C. Paranicas[4], D. Ranquist[3], M. Reno[11], M. F. Thomsen[12], P. W. Valek[1,2], S. Weidner[10], and R. J. Wilson[3]

[1]Southwest Research Institute, San Antonio, Texas, USA, [2]Department of Physics and Astronomy, University of Texas at San Antonio, San Antonio, Texas, USA, [3]Laboratory for Atmospheric and Space Physics, University of Colorado Boulder, Boulder, Colorado, USA, [4]The Johns Hopkins University Applied Physics Laboratory, Laurel, Maryland, USA, [5]Goddard Space Flight Center, Greenbelt, Maryland, USA, [6]Department of Physics and Astronomy, University of Iowa, Iowa, USA, [7]Jet Propulsion Laboratory, California, USA, [8]Institut de Recherche en Astrophysique et Planétologie, Toulouse, France, [9]Department of Astrophysical Sciences, Princeton University, Princeton, New Jersey, USA, [10]Office of the VP for the Princeton Plasma Physics Laboratory, Princeton University, Princeton, New Jersey, USA, [11]Austin Mission Consulting, Austin, Texas, USA, [12]Planetary Science Institute, Tucson, Arizona, USA

Key Points:
- Juno/JADE made high temporal resolution measurements at high latitudes of the Io torus and plasma sheet plasma populations
- We identify regions where Juno was connected to the Io torus, inner plasma sheet, middle plasma sheet, outer plasma sheet, and high-latitude polar region
- For JADE's first auroral transits at ~0.7 R_J altitude and <100 keV, we find no evidence for a broad Jovian auroral acceleration region

Correspondence to:
J. R. Szalay,
jszalay@swri.edu

Citation:
Szalay, J. R., et al. (2017), Plasma measurements in the Jovian polar region with Juno/JADE, *Geophys. Res. Lett.*, *44*, 7122–7130, doi:10.1002/2017GL072837.

Received 1 FEB 2017
Accepted 28 MAR 2017
Published online 27 JUL 2017

Abstract Jupiter's main auroral oval provides a window into the complex magnetospheric dynamics of the Jovian system. The Juno spacecraft entered orbit about Jupiter on 5 July 2016 and carries on board the Auroral Distributions Experiment (JADE) that can directly sample the auroral plasma structures. Here we identify five distinct regimes in the JADE data based on composition/energy boundaries and magnetic field mappings, which exhibit considerable symmetry between the northern and southern passes. These intervals correspond to periods when Juno was connected to the Io torus, inner plasma sheet, middle plasma sheet, outer plasma sheet, and the polar region. When connected to the torus and inner plasma sheet, the heavy ions are consistent with a corotating pickup population. For Juno's first perijove, we do not find evidence for a broad auroral acceleration region at Jupiter's main auroral oval for energies below 100 keV.

1. Introduction

Many of the auroral signatures observed throughout the solar system are attributed to accelerated electrons interacting with a planet's atmosphere. Aurorae have been most extensively studied at Earth, with sounding rockets and multiple orbiting spacecraft [*Evans*, 1974, *Mozer et al.*, 1977, *Carlson et al.*, 1998]. At Earth, a host of auroral phenomena have been observed including parallel electric fields (double layers), perpendicular electrostatic shocks, accelerated electrons, anti-earthward ion beams, strong wave activity, and deep density cavities [*Mauk and McIlwain*, 1975; *Sharp et al.*, 1975; *Klumpar et al.*, 1976; *Ergun et al.*, 1998, 2000, 2002, 2004]. While Jupiter's plasma environment is significantly different from Earth's, similar auroral processes have been posited to occur at Jupiter [*Barbosa et al.*, 1981; *Cowley and Bunce*, 2001; *Nichols and Cowley*, 2004; *Clarke et al.*, 2004; *Ray et al.*, 2009, 2010, 2012].

In the Jovian magnetosphere, neutrals are emitted from Io; a large fraction of these neutrals are subsequently ionized via charge exchange and electron impact, generating fresh plasma that is picked up and moves with the corotating plasma. These iogenic plasma populations make up the Jovian plasma sheet, a reservoir of plasma mostly confined to a region near the magnetic equatorial plane. In situ measurements in the plasma sheet showed the ionic composition to be dominated by $M/q = 16$, with O^+ and/or S^{++} ions as the dominant population [e.g., *McNutt et al.*, 1981]. As plasma is transported radially outward, conservation of angular momentum dictates that it must slow down relative to corotation. Maintaining rigid corotation requires Jupiter's ionosphere to provide the needed angular momentum. It is argued this is done through a current system whereby a $\mathbf{J} \times \mathbf{B}$ torque acts on the equatorial plasma. This process begins to break down at large radial distances, where the finite ionospheric conductivity inhibits the generation of large currents required to fully transfer the angular momentum needed to bring rotating plasma up to full corotation [*Hill*, 1979]. It is hypothesized that the region of corotation breakdown (or flow shear) is linked to auroral emissions [*Hill*, 2001].

The aurorae at Jupiter provide a window into this complex current system. The Juno mission is a polar-orbiting spacecraft, which entered orbit about Jupiter on 5 July 2016 (UTC). One of Juno's primary mission

objectives is to explore the polar magnetosphere and aurorae [*Bagenal et al*., 2014]. On board, it carries the Jovian Auroral Distributions Experiment (JADE), an instrument suite that consists of a single ion detector, JADE-I (0.01–50 keV/*q*), and two electron detectors, JADE-E (0.1–100 keV) [*McComas et al*., 2013]. Prior to Juno's first science perijove pass, JADE measured the inbound solar wind, magnetosheath, and magnetosphere [*McComas et al*., 2017], observed a hot flow anomaly [*Valek et al*., 2017], found evidence for magnetic reconnection at the magnetopause [*Ebert et al*., 2017], observed mass transport across the magnetopause [*Gershman et al*., 2017], and found evidence for a connection between solar wind inputs and auroral emissions [*Nichols et al*., 2017].

Here we describe the JADE measurements taken during Juno's rapid transit between the northern and southern regions of Jupiter's polar magnetosphere on the dusk side during Juno's first science perijove. In section 2, we briefly describe the magnetic field mapping schemes used. In section 3, we characterize the plasma measurements taken on close approach by relating them to their magnetospheric sources and auroral mappings. We conclude in section 4 with a discussion of the contrast between our expectations of the structure of the Jovian auroral current system and the JADE measurements.

2. Magnetic Field Mapping

The Jovian literature commonly uses "L shell" to identify the equatorial crossing distance of a dipolar magnetic field line. This value is convenient for relating spacecraft measurements at high latitudes to their equatorially mapped source regions. Since the Jovian field is very stretched, the use of a dipole L shell for organizing measurements can be misleading. To reduce ambiguity, we adopt the terminology "M shell" (M for magnetic) to describe the equatorial crossing distances for any given field line. We use the VIP4+CAN magnetic field models [*Connerney et al*., 1981, 1998], a synthesis of a multipole internal field model (VIP4) and current sheet model (CAN), to determine M shells for magnetic field lines crossing through Juno in this work. This model is typically applicable for mappings to $6 < M < 30\ R_J$ and less accurate in mapping field lines very near to the northern auroral kink region [*Vogt et al*., 2015]. We note that M shell mapping is not strictly constant in time, changing with variations in the plasma conditions within the magnetosphere [*Nichols*, 2011; *Nichols et al*., 2015]; however, we assume time-invariant mappings for simplicity in this work.

M shell ranges for the Jovian auroral oval have been estimated via a variety of techniques. One of the more stringent constraints on the oval mapping distance is the observation of Ganymede's auroral foot point, which typically occurs equatorward of the main oval. Since Ganymede orbits at 15 R_J, this puts an approximate lower limit on the inner M shell of the oval at $M > 15\ R_J$ [*Clarke et al*., 2002], though the latitudinal gap between the foot point and edge of the auroral oval suggests an inner edge closer to 20–30 R_J. We note that there have been outlying events during which the Ganymede footprint was transiently equatorward of the main auroral emission [*Bonfond et al*., 2012]. Separate modeling efforts have also concluded that the source region for the auroral oval begins around $M = 20$–$30\ R_J$ and extends to several tens of R_J beyond that distance [e.g., *Hill*, 2001; *Cowley and Bunce*, 2001; *Nichols*, 2011; *Vogt et al*., 2011].

3. High-Latitude Observations

During the 6 h centered about Juno's perijove, JADE took measurements in its high-rate science mode, with 1 s resolution for JADE-E and 2 s resolution for JADE-I. Approaching the northern pole from the dawnside, JADE was magnetically connected to the polar auroral region. Here JADE experienced large intermittent bursts of penetrating radiation and, with the exception of a few periods, measured ion and electron populations with very low densities within the JADE energy range. However, as Juno's planetary footprint moved equatorward, JADE observed a diverse and complex plasma environment, with significant structure on a variety of timescales. Here we identify five distinct boundaries in the JADE data, corresponding to five separate plasma regimes that exhibit considerable symmetry between the northern and southern passes. To identify boundaries, we analyze the electron and heavy ion data. Unlike protons, heavy ions such as O and S, in high relative numbers, suggest magnetospheric (i.e., not Jovian, sheath, or solar wind) populations. We therefore favor these populations over the proton data to identify distinct plasma boundaries relating to the magnetic field mapping. Figure 1 summarizes the JADE measurements during closest approach, with the separate regions discussed below in order of increasing M shell. Note, in this work, that we performed a preliminary

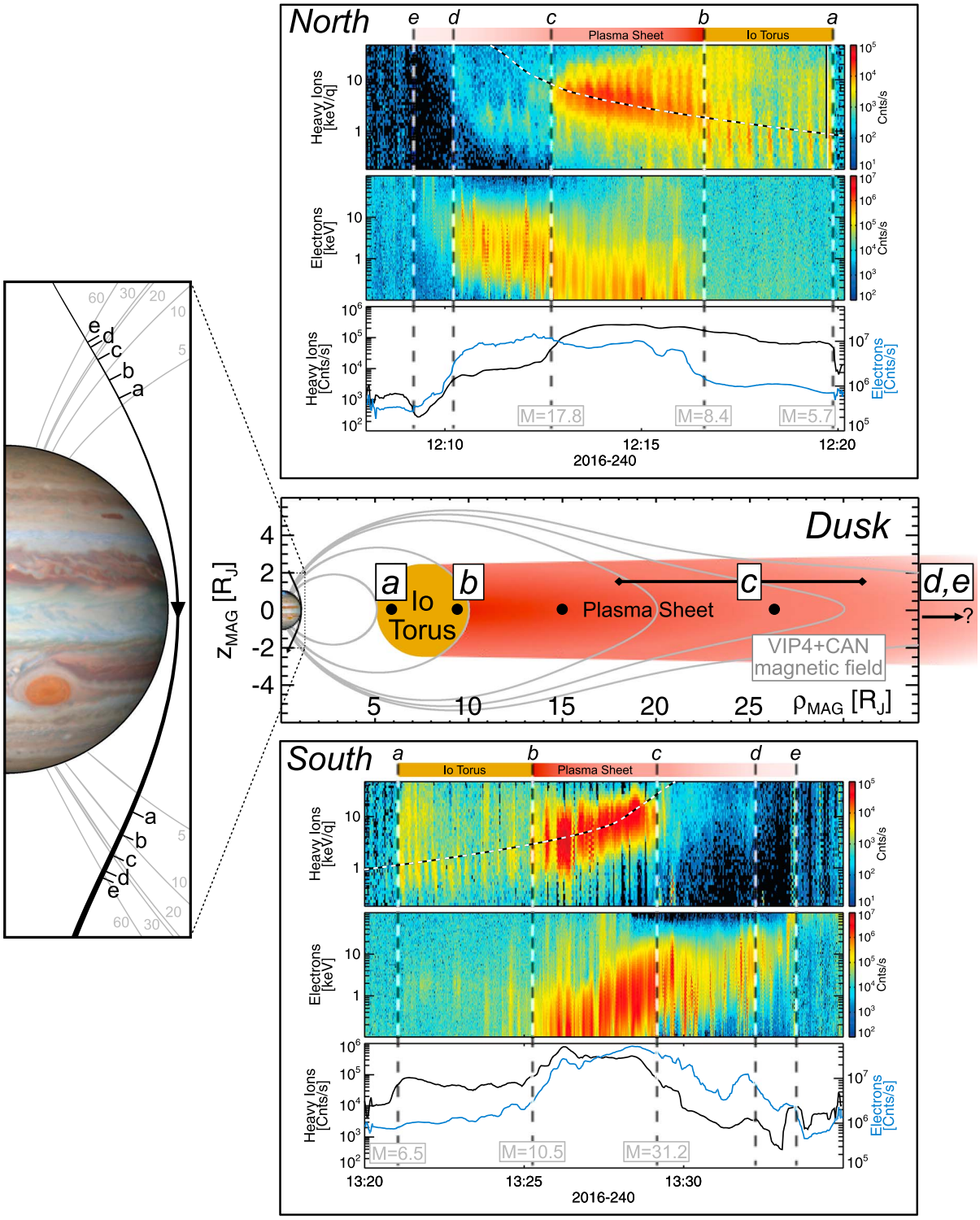

Figure 1. Summary of the JADE heavy ion ($M/q \geq 8$) and electron measurements, with energy versus time spectrograms and total count rates, taken during the northern and southern (N/S) polar passes of Juno's first science perijove. We identify distinct periods for both the N/S passes in which Juno was connected to the Io torus and plasma sheet. The heavy ion panels indicate twice the equatorial corotational energy for M/q = 16 (dashed line). The left and middle panels show the overall measurement geometry and VIP4+CAN magnetic field model [*Connerney et al.*, 1981, 1998]. Black dots indicate the locations of the four Galilean moons, in order of increasing radial distance from Jupiter: Io, Europa, Ganymede, and Callisto.

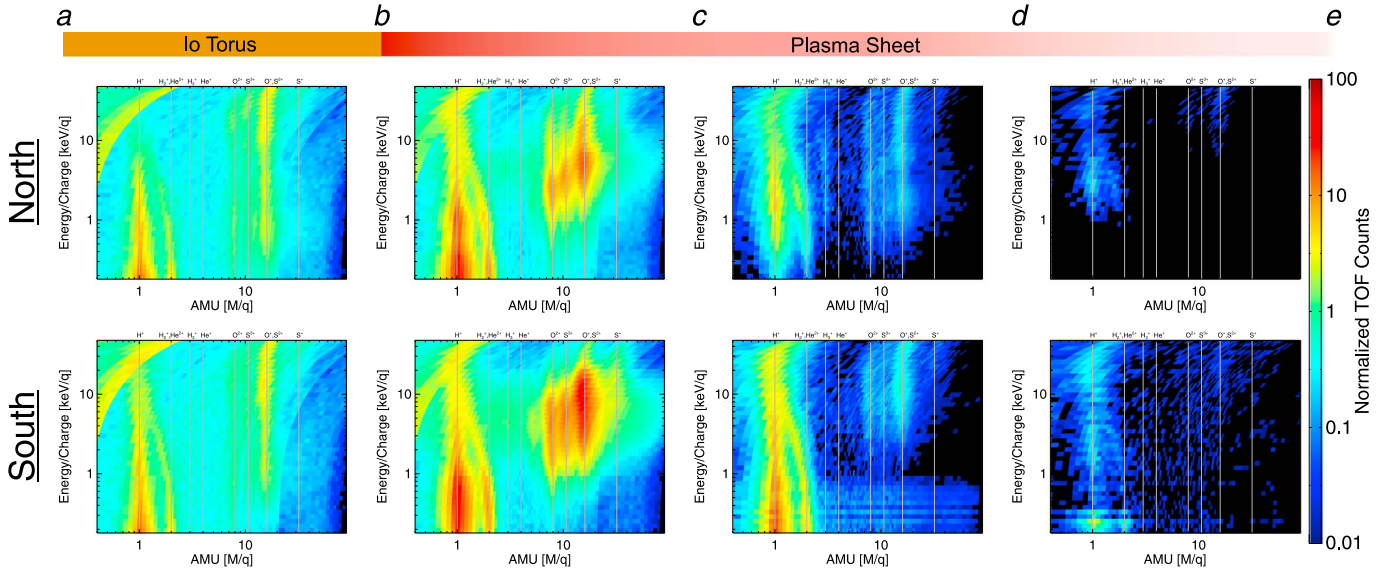

Figure 2. *M/q* versus energy from JADE-I for the northern and southern inner magnetosphere measurements near Juno's periojove. Count rates are all normalized to the same scale. The Io torus populations observed at high latitudes exhibit broad energy structures with the majority of heavy ion counts dominated by $M/q = 16$ corresponding to O^+ or S^{++}. JADE plasma sheet measurements show significant energetic populations of O^{++}, S^{+++}, and O^+/S^{++} and a smaller contribution from S^+.

background subtraction to the JADE-I and JADE-E data based on the use of the background anodes [*McComas et al.*, 2013].

Boundary (a) maps to M shell values of 5.7 R_J (north) and 6.5 R_J (south), with boundary (b) mapping to 8.4 R_J (north) and 10.5 R_J (south). When connected to M shells inside of (a), JADE experienced large fluxes of penetrating radiation due to the radiation belts [*Paranicas et al.*, 2017] with little indication of a low-energy plasma population within the JADE energy ranges above noise levels. Between (a) and (b), JADE measured heavy ion populations dominated by $M/q = 16$, corresponding to O^+ and/or S^{++} that spanned an energy range of a few hundred eV to tens of keV, up to the top of the JADE-I measurement range (Figure 2). There are no distinct electron populations in the JADE-E instrument range measured in the northern pass for this region, with evidence for a very low density electron population with energies between 0.1 and a few keV in the south. The heavy ion time-energy spectrograms show a large degree of spin modulation during this time interval, indicating that these ion populations are highly directional. The compositional dominance of $M/q = 16$ and dearth of electrons >100 eV is consistent with previous spacecraft measurements in the Io torus [*Bagenal and Sullivan*, 1981; *Sittler and Strobel*, 1987]. Additionally, the M shell mappings for this region are consistent with the Io torus boundaries. Therefore, we interpret this region physically as being connected to the Io torus. We note that a high-energy population of heavy ions with characteristic energy of 10–20 keV was observed on the northern pass when transitioning past boundary (b), yet not in the southern pass.

Near boundary (b), JADE observed a rapid increase in the total count rates of heavy ions. Based on the trend line, this is the location where the plasma electrons become hot enough to be observed by JADE-E; presumably, they are cooler in region between (a) and (b). The ions are notably more isotropic, as the spin modulation signature is less pronounced. As (b) maps to M shells consistent with the outer edge of the Io torus, we interpret the region bounded by (b) and (c) to be connected to the inner plasma sheet (boundary (c) described below). The heavy ion panels in Figure 1 show twice the equatorial corotation energy (dotted line) for the dominant $M/q = 16$ species, which correlates well with the peak in the count rate spectrogram between (b) and (c). For a subthermal Maxwellian distribution, the peak in the count rate spectrogram will occur at twice the thermal energy (with minor energy-dependent corrections). Therefore, the heavy ions observed in this period are preliminarily consistent with a corotating population from the inner plasma sheet, heated via a process that scales with corotation energy. Additionally, significant energetic populations of O^{++}, S^{+++}, O^+, and/or S^{++}, and a smaller contribution from S^+, were observed, consistent with an inner plasma sheet source (Figure 2).

Table 1. Locations and Geometric Information for the 10 Boundaries Identified in the JADE PJ1 Close Approach Data[a]

	N/S	Time (UTC)	R (R_J)	LT (hh:mm)	M (R_J)	λ_{III} (deg)	θ_{III} (deg)	θ_{MAG} (deg)	θ_{CEN} (deg)
a	N	2016-240T12:19:53	1.47	17:51	5.7	77.5	67.8	61.6	63.9
a	S	2016-240T13:21:03	1.45	17:53	6.5	113.9	−59.6	−57.8	−58.7
b	N	2016-240T12:16:36	1.54	17:50	8.4	75.6	72.1	65.4	67.9
b	S	2016-240T13:25:16	1.55	17:53	10.5	116.3	−65.1	−62.6	−63.8
c	N	2016-240T12:12:43	1.63	17:50	17.8	73.4	76.6	69.4	72.1
c	S	2016-240T13:29:09	1.63	17:54	31.2	118.6	−69.6	−66.4	−67.9
d	N	2016-240T12:10:13	1.68	17:49	52.0	72.0	79.3	71.8	74.5
d	S	2016-240T13:32:15	1.71	17:54	58.8	120.4	−72.8	−69.1	−70.8
e	N	2016-240T12:09:12	1.71	17:49	57.3	71.5	80.3	72.7	75.5
e	S	2016-240T13:33:32	1.74	17:54	62.9	121.2	−74.1	−70.1	−71.9

[a]Columns show the boundary label, northern/southern hemisphere, time in UTC, radial distance of Juno from the center of Jupiter, local time (LT) of Juno, M shell, System III longitude (left handed), System III latitude, VIP4 dipole magnetic latitude, and VIP4 dipole centrifugal latitude.

Boundary (c) is of particular interest as it maps to the middle plasma sheet, with M shells of 17.8 R_J (north) and 31.2 R_J (south) where the literature would suggest the inner edge of the main auroral oval maps to [e.g., *Hill*, 2001; *Cowley and Bunce*, 2001; *Clarke et al*., 2002; *Nichols*, 2011; *Vogt et al*., 2011]. We note that the lower of the two M shells for boundary (c), 17.8 R_J, is the mapped value from the northern hemisphere near the kink region. Given the putative magnetic anomaly in this region [*Grodent et al*., 2008], M shell mappings near it are particularly error prone [*Vogt et al*., 2015]. We therefore favor the southern mapped boundary for (c) of 31.2 R_J and suggest that this is closer to the true equatorial mapping distance. In general, we expect all of the given M shells to be more accurate for the southern pass during these observations for the same reason. In transitioning past boundary (c), the heavy ions are observed to have a rapid decrease in total counts, with peak energies that no longer follow the corotational energy and consistent with increasingly large corotation lag. Some part of the reduction in heavy ion counts in the (c)-(d) region may also be attributable to the much increased influence of the centrifugal confinement at the large radial distances to which this region maps. Additionally, the electron energies are marked by a sharp jump in energy to a few keV at boundary (c). We hypothesize that the region bounded by (c) and (d), which maps to the middle plasma sheet and is characteristically different than the adjacent inner plasma sheet connected region, corresponds to the main auroral oval region (see also the ionospheric mapping discussion below). More detailed analysis of the JADE-E data indicates that the low-energy electron population in this region is primarily moving upward (small local pitch angle) [*Allegrini et al*., 2017]. While the tentative identification of the main oval region is based on geometric constraints discussed throughout this work, we note that the character of the electrons measured by JADE is not conclusively consistent with the presence of a population of primarily downward accelerated electrons [*Allegrini et al*., 2017].

The region bounded by (d) and (e) is characterized by an additional decrease in the heavy ion and electron counts by an order of magnitude. The electrons' energies continue to increase up to boundary (e) at which point there is an abrupt cutoff of the electron population that is also observed in the high-energy plasma populations by JEDI [*Mauk et al*., 2017]. We interpret this region to be connected to the outer plasma sheet, past the main auroral current system, with boundary (d) defining the poleward edge of the main auroral oval. Past (e), the JADE measurements for both ions and electrons are dominated by penetrating radiation, which manifests itself in JADE measurements as vertical strips with similar count rates throughout the energy range. Aside from these radiation signatures, the ion and electron populations exhibit very low densities. Table 1 summarizes the five boundaries and gives relevant geometric quantities.

In addition to identifying how these measurements relate to magnetospheric sources, we now discuss the mapping of Juno's magnetic footprint onto the Jovian ionosphere. Figure 3 shows Juno's trajectory mapped onto the ionosphere using the VIP4 model. The blue dotted/solid lines show the mean auroral boundaries/center from a statistical study of Hubble Space Telescope (HST) observations from 2007 [*Nichols et al*., 2009; *Bonfond et al*., 2012]. We have also included a grid (grey) that runs tangent to the mean oval to provide a reference to the distances traversed. In this figure, we have identified the five boundaries for both the northern and southern passes.

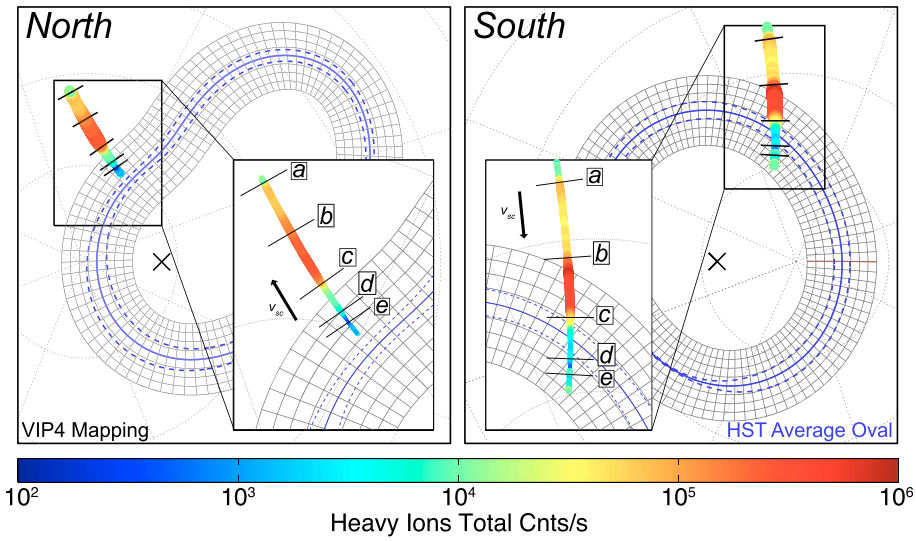

Figure 3. Mapping of the Juno trajectory during the PJ1 close approach with the VIP4 magnetic field model [*Connerney et al.*, 1998]. Both projections are shown as viewed from above the north pole. The blue solid/dotted lines indicate the average center and boundaries for the auroral oval based on HST observations [*Bonfond et al.*, 2012]. The longitudinal gridlines (grey) parallel to the mean oval are spaced in increments of 1250 km on the 1 bar level from the mean oval. The intersection of the north and south VIP4 magnetic dipole moment with the Jovian surface is marked with a cross.

For the southern hemisphere, the predicted oval crossing times coincide remarkably well with our identified auroral region, as evidenced by the proximity of boundaries (c) and (d) to the statistical average oval boundaries. However, in the northern hemisphere, the JADE identified that auroral region is well equatorward of the main average oval. We attribute this offset to two reasons. First, the VIP4 model is less reliable when mapping magnetic field lines near the kink region, which Juno flew directly over, making estimation of the true footprint less accurate. Second, both the northern and southern passes were made very near to the dusk terminator. The auroral emissions have been observed to be asymmetric in local time, with the dusk emissions notably variable and more extended [*Bonfond et al.*, 2015], due to the local time dependence in Jupiter's magnetospheric plasma structures. Additionally, during the time leading up to the flyby, HST measurements observed the dusk northern auroral oval to be equatorward of the 2007 statistical average oval [*Nichols et al.*, 2017], qualitatively consistent with the JADE measurements. We suggest that these explanations account for the discrepancy between the northern and southern auroral mappings.

The pattern and sequence of features in the north and south are very similar, lending credence to the interpretation that these periods map to similar magnetospheric regions. Our position is that the data are more indicative of regions than model-dependent mappings. Given the more accurate mapping to the main oval in the south, which well correlates to specific features in the JADE data, we therefore infer the oval location in the north based on the strong symmetry in data features.

4. Discussion and Conclusions

Juno moves from north to south close to the planet; hence, JADE passes rapidly through field lines whose equatorial crossing points probably span tens of R_J's in equatorial space. To interpret these data, we have identified five distinct regions in the JADE heavy ion and electron data, which we posit physically map to the Io torus, inner plasma sheet, middle plasma sheet, outer plasma sheet, and the high-latitude polar region. We note that this work focuses on the lower energy plasma populations within the JADE energy range, where the energetic plasma populations are discussed in other studies in this issue [*Clark et al.*, 2017; *Haggerty et al.*, 2017; *Kollmann et al.*, 2017; *Mauk et al.*, 2017]. In this study, high densities of electrons, oxygen, and sulfur and their variation with energy and intensity are used as discriminators between different magnetospheric and other regions. The regions are identified in the data by energy/composition boundaries,

and their physical interpretation is guided by their magnetic field mappings. Due to the magnetic anomaly in Jupiter's northern hemisphere, we have relied more heavily on the southern hemisphere data set for mapping purposes.

In the region connected to the Io torus and plasma sheet, heavy ions (primarily O^+ and/or S^{++}) have observed energies consistent with corotation of ions picked up in the near-equatorial region. The presence of such ions at these high latitudes suggests that there is a robust process of pitch angle scattering that enables particles picked up with equatorial pitch angles near 90° to travel to the spacecraft without mirroring.

Some of the most intriguing features of the JADE measurements are the characteristic ion and electron energies when connected to the middle plasma sheet and likely to the main oval. Electrons in the middle magnetosphere have suprathermal energies ~2.5 keV [*Scudder et al*., 1981]. The bright auroral features are consistent with an electron population with energies of ~20–400 keV, derived both from modeling and observational efforts [*Cowley and Bunce*, 2001; *Saur et al*., 2003; *Nichols and Cowley*, 2004; *Gustin et al*., 2004, 2016]. To reconcile the discrepancy between the low energies in the magnetospheric source region and the large electron energies needed to create the aurora, large parallel electric fields with potentials of 20–400 keV have been posited to exist at distances of a few Jovian radii from the ionosphere [*Ray et al*., 2009, 2010, 2012]. We note that many of these models use postmidnight configurations of the magnetic field and that focused modeling efforts on the local time dependence of auroral emissions suggest lower field-aligned current densities and precipitating auroral energy fluxes at dusk [*Ray et al*., 2014]. Measurements through auroral acceleration regions at Earth were observed to have an "inverted-V" structure in the time-energy spectrograms. This structure was interpreted as a peak in the field-aligned potential drop in the center of the auroral acceleration region, which decreased on the edges of these regions [*Lyons et al*., 1979; *Lyons* 1980, 1981]. Multiple simulations of the Jovian auroral currents predict that a similar structure exists connected to Jupiter's main oval, where a peak in the acceleration potential exists in the middle of the auroral oval [*Cowley and Bunce*, 2001; *Nichols and Cowley*, 2004, 2005; *Ray et al*., 2010, 2012]. Voyager 1 plasma wave measurements consistent with field-aligned currents between 10 and 30 R_J near the plasma sheet have also suggested the existence of inverted-V electrons at high latitudes in the Jovian magnetosphere due to field-aligned potential drops [*Barbosa et al*., 1981].

However, during the period we attribute to the main auroral current region, when Juno was at planetocentric distances of 1.6–1.7 R_J such that it should be below the putative acceleration region posited to exist at distances >2 R_J [*Cowley and Bunce*, 2001; *Su et al*., 2003; *Ray et al*., 2009], the electron time-energy spectrograms do not indicate broad-scale inverted-V structures spanning the entire auroral region within the JADE energy range. Instead, the electron energies measured are typical of the magnetospheric electrons in the plasma sheet and not of a population accelerated over tens to hundreds of keV. Additionally, were Juno to have flown under an auroral acceleration region with potentials of 20–400 keV, the heavy ions originating in the plasma sheet with energies below the auroral acceleration potential would never be able to overcome this potential and reach the JADE instrument. The detection of one to tens of keV/q heavy ions at such close-in distances is not consistent with Juno having flown under a broad auroral acceleration region for this orbit.

In fact, a large population of the electrons is actually moving away from Jupiter, suggesting a lower altitude electron source [*Allegrini et al*., 2017; *Mauk et al*., 2017]. If a broad auroral acceleration region exists with strong anti-Jovian electric fields and is located at distances less than 1.6 R_J, such that Juno flew above this region, the upward moving electrons from the ionosphere with energies below the acceleration potential would never be able to reach Juno given the large predicted potential barrier of 20–400 keV they would transit. Even with a single perijove of plasma measurements, these observations signal us to reconsider our notions of how auroral current systems are structured in the Jovian system, particularly with respect to broad auroral acceleration regions.

Poleward of the main auroral current region, at higher latitudes past boundary (e), while JADE primarily registers counts from penetrating radiation, plasma populations above the JADE instrument range were observed [*Mauk et al*., 2017]. These polar measurements either map to the outermost region of the magnetosphere or could be connected to the solar wind. Constraining the location of the polar region boundary, tightening the definition of this region, and further constraining the boundaries outlined in this work will benefit from a cross comparison between multiple instruments on the Juno payload in future studies.

Lastly, we note that while Juno dips into the dawnside plasma sheet numerous times during the outer portions of its orbit (with limited early JADE measurements), it never directly samples the duskside plasma sheet. Due to the rotationally driven dynamics of the Jovian magnetosphere, there is a large degree of local time asymmetry in the plasma sheet [*Kivelson and Khurana*, 2002; *Vogt et al.*, 2011]. The dusk plasma sheet has been measured to be much thicker than that of the dawnside, due to the extreme heating that takes place in the afternoon sector [*Kivelson and Southwood*, 2005]. Additionally, the morning side "cushion" region between the outer plasma sheet and magnetopause was never observed on the duskside [*Khurana et al.*, 2004]. These local time asymmetries make relating distant dawnside plasma sheet measurements to the close in duskside auroral measurements difficult. However, as Juno's orbit precesses with perijove moving from dusk toward noon, the close-in auroral measurements will correspondingly map from the dusk plasma sheet toward the noon plasma sheet, allowing JADE to sample and characterize a diverse range of magnetospheric auroral source regions.

Acknowledgments
The authors would like to thank the many JADE and Juno team members that made these observations possible. The JADE datum used for this study was the JNO-J/SW-JAD-3-CALIBRATED-V1.0 data set, which was obtained from the Planetary Data System (PDS) at http://pds.nasa.gov/. Juno contract NNM06AA75C.

References

Allegrini, F., et al. (2017), Electron beams and loss cones in the auroral regions of Jupiter, *Geophys. Res. Lett.*, *44*, 7131–7139, doi:10.1002/2017GL073180.

Bagenal, F., and J. D. Sullivan (1981), Direct plasma measurements in the Io torus and inner magnetosphere of Jupiter, *J. Geophys. Res.*, *86*, 8447–8466, doi:10.1029/JA086iA10p08447.

Bagenal, F., et al. (2014), Magnetospheric science objectives of the Juno mission, *Space Sci. Rev.*, 1–69, doi:10.1007/s11214-014-0036-8.

Barbosa, D. D., F. L. Scarf, W. S. Kurth, and D. A. Gurnett (1981), Broadband electrostatic noise and field-aligned currents in Jupiter's middle magnetosphere, *J. Geophys. Res.*, *86*, 8357–8369, doi:10.1029/JA086iA10p08357.

Bonfond, B., D. Grodent, J.-C. Gérard, T. Stallard, J. T. Clarke, M. Yoneda, A. Radioti, and J. Gustin (2012), Auroral evidence of Io's control over the magnetosphere of Jupiter, *Geophys. Res. Lett.*, *39*, L01105, doi:10.1029/2011GL050253

Bonfond, B., J. Gustin, J.-C. Gérard, D. Grodent, A. Radioti, B. Palmaerts, S. Badman, K. Khurana, and C. Tao (2015), The far-ultraviolet main auroral emission at Jupiter—Part 1: Dawn-dusk brightness asymmetries, *Ann. Geophys.*, *33*, 1203–1209.

Carlson, C. W., et al. (1998), FAST observations in the downward auroral current region: Energetic upgoing electron beams, parallel potential drops, and ion heating, *Geophys. Res. Lett.*, *25*, 2017–2020, doi:10.1029/98GL00851.

Clark, G., et al. (2017), Observation and interpretation of energetic ion conics in Jupiter's polar magnetosphere, *Geophys. Res. Lett.*, doi:10.1002/2016GL072325, in press.

Clarke, J. T., et al. (2002), Ultraviolet emissions from the magnetic footprints of Io, Ganymede and Europa on Jupiter, *Nature*, *415*, 997–1000.

Clarke, J. T., D. Grodent, S. W. H. Cowley, E. J. Bunce, P. Zarka, J. E. P. Connerney, and T. Satoh (2004), Jupiter's aurora, in *Jupiter: The Planet, Satellites and Magnetosphere*, vol. 1, edited by F. Bagenal, T. E. Dowling, and W. B. McKinnon, pp. 639–670, Cambridge Univ. Press, New York.

Connerney, J. E. P., M. H. Acuna, and N. F. Ness (1981), Modeling the Jovian current sheet and inner magnetosphere, *J. Geophys. Res.*, *86*, 8370–8384, doi:10.1029/JA086iA10p08370.

Connerney, J. E. P., M. H. Acuna, N. F. Ness, and T. Satoh (1998), New models of Jupiter's magnetic field constrained by the Io flux tube footprint, *J. Geophys. Res.*, *103*, 11,929–11,940, doi:10.1029/97JA03726.

Cowley, S. W. H., and E. J. Bunce (2001), Origin of the main auroral oval in Jupiter's coupled magnetosphere–ionosphere system, *Planet. Space Sci.*, *49*, 1067–1088.

Ebert, R. W., et al. (2017), Accelerated flows at Jupiter's magnetopause: Evidence for magnetic reconnection along the dawn flank, *Geophys. Res. Lett.*, *44*, 4401–4409, doi:10.1002/2016GL072187.

Ergun, R. E., et al. (1998), FAST satellite observations of electric field structures in the auroral zone, *Geophys. Res. Lett.*, *25*, 2025–2028, doi:10.1029/98GL00635.

Ergun, R. E., C. W. Carlson, J. P. McFadden, F. S. Mozer, and R. J. Strangeway (2000), Parallel electric fields in discrete arcs, *Geophys. Res. Lett.*, *27*, 4053–4056, doi:10.1029/2000GL003819.

Ergun, R. E., L. Andersson, D. S. Main, Y.-J. Su, C. W. Carlson, J. P. McFadden, and F. S. Mozer (2002), Parallel electric fields in the upward current region of the aurora: Indirect and direct observations, *Phys. Plasmas*, *9*, 3685–3694.

Ergun, R. E., L. Andersson, D. Main, Y.-J. Su, D. L. Newman, M. V. Goldman, C. W. Carlson, A. J. Hull, J. P. McFadden, and F. S. Mozer (2004), Auroral particle acceleration by strong double layers: The upward current region. *J. Geophys. Res.*, *109*, A12220, doi:10.1029/2004JA010545.

Evans, D. S. (1974), Precipitating electron fluxes formed by a magnetic field aligned potential difference, *J. Geophys. Res.*, *79*, 2853–2858, doi:10.1029/JA079i019p02853.

Gershman, D. J., et al. (2017), Juno observations of large-scale compressions of Jupiter's dawnside magnetopause, *Geophys. Res. Lett.*, doi:10.1002/2017GL073132, in press.

Grodent, D., B. Bonfond, J.-C. Gérard, A. Radioti, J. Gustin, J. T. Clarke, J. Nichols, and J. E. P. Connerney (2008), Auroral evidence of a localized magnetic anomaly in Jupiter's northern hemisphere. *J. Geophys. Res.*, *113*, A09201, doi:10.1029/2008JA013185.

Gustin, J., J.-C. Gérard, D. Grodent, S. W. H. Cowley, J. T. Clarke, and A. Grard (2004), Energy-flux relationship in the FUV Jovian aurora deduced from HST-STIS spectral observations, *J. Geophys. Res.*, *109*, A10205, doi:10.1029/2003JA010365.

Gustin, J., D. Grodent, L. C. Ray, B. Bonfond, E. J. Bunce, J. D. Nichols, N. Ozak (2016), Characteristics of north Jovian aurora from STIS FUV spectral images, *Icarus*, *268*, 215–241.

Haggerty, D. K., B. H. Mauk, C. P. Paranicas, G. Clark, P. Kollmann, A. M. Rymer, S. J. Bolton, J. E. P. Connerney, and S. M. Levin (2017), Juno/JEDI observations of 0.01 to >10 MeV energetic ions in the Jovian auroral regions: Anticipating a source for polar X-ray emission, *Geophys. Res. Lett.*, doi:10.1002/2017GL072866, in press.

Hill, T. W. (1979), Inertial limit on corotation, *J. Geophys. Res.*, *84*, 6554–6558.

Hill, T. W. (2001), The Jovian auroral oval, *J. Geophys. Res.*, *106*, 8101–8108, doi:10.1029/2000JA000302.

Khurana, K. K., M. G. Kivelson, V. M. Vasyliunas, N. Krupp, J. Woch, A. Lagg, B. H. Mauk, and W. S. Kurth (2004), The configuration of Jupiter's magnetosphere, in *Jupiter. The Planet*, edited by F. Bagenal, T. E. Dowling, and W. B. McKinnon, pp. 593–616, Cambridge Univ. Press, Cambridge, U. K.

Kivelson, M. G., and K. K. Khurana (2002), Properties of the magnetic field in the Jovian magnetotail, *J. Geophys. Res.*, *107*(A8), SMP 23-1–SMP 23-9, doi:10.1029/2001JA000249.

Kivelson, M. G., and D. J. Southwood (2005), Dynamical consequences of two modes of centrifugal instability in Jupiter's outer magnetosphere, *J. Geophys. Res.*, *110*, A12209, doi:10.1029/2005JA011176.
Klumpar, D. M., J. R. Burrows, and M. D. Wilson (1976), Simultaneous observations of field-aligned currents and particle fluxes in the post-midnight sector, *Geophys. Res. Lett.*, *3*, 395–398, doi:10.1029/GL003i007p00395.
Kollmann, P., et al. (2017), A heavy ion and proton radiation belt inside of Jupiter's rings, *Geophys. Res. Lett.*, *44*, 5259–5268, doi:10.1002/2017GL073730.
Lyons, L. R. (1980), Generation of large–scale regions of auroral currents, electric potentials, and precipitation by the divergence of the convection electric field, *J. Geophys. Res.*, *85*(A1), 17–24, doi:10.1029/JA085iA01p00017.
Lyons, L. R. (1981), Discrete aurora as the direct result of an inferred high-altitude generating potential distribution, *J. Geophys. Res.*, *86*(A1), 1–8, doi:10.1029/JA086iA01p00001.
Lyons, L. R., D. S. Evans, and R. Lundin (1979), An observed relationship between magnetic field-aligned electric fields and downward electron energy fluxes in the vicinity of auroral forms, *J. Geophys. Res.*, *84*, 457–461, doi:10.1029/JA084iA02p00457.
Mauk, B. H., and C. E. McIlwain (1975), ATS-6 UCSD Auroral Particles Experiment, *IEEE Trans. Aerosp. Electron. Syst.*, *11*, 1125–1130.
Mauk, B. H., et al. (2017), Juno observations of energetic charged particles over Jupiter's polar regions: Analysis of monodirectional and bidirectional electron beams, *Geophys. Res. Lett.*, *44*, 4410–4418, doi:10.1002/2016GL072286.
McComas, D. J., et al. (2013), The Jovian Auroral Distributions Experiment (JADE) on the Juno mission to Jupiter, *Space Sci. Rev.*, 1–97, doi:10.1007/s11214-013-9990-9.
McComas, D. J., et al. (2017), Plasma environment at the dawn flank of Jupiter's magnetosphere: Juno arrives at Jupiter, *Geophys. Res. Lett.*, *44*, 4432–4438, doi:10.1002/2017GL072831.
McNutt, R. L., Jr., J. W. Belcher, and H. S. Bridge (1981), Positive ion observations in the middle magnetosphere of Jupiter, *J. Geophys. Res.*, *86*, 8319–8342, doi:10.1029/JA086iA10p08319.
Mozer, F. S., C. W. Carlson, M. K. Hudson, R. B. Torbert, B. Parady, J. Yatteau, and M. C. Kelley (1977), Observations of paired electrostatic shocks in the polar magnetosphere, *Phys. Rev. Lett.*, *38*, 292–295.
Nichols, J. D. (2011), Magnetosphere-ionosphere coupling in Jupiter's middle magnetosphere: Computations including a self-consistent current sheet magnetic field model, *J. Geophys. Res.*, *116*, A10232, doi:10.1029/2011JA016922.
Nichols, J. D., and S. W. H. Cowley (2004), Magnetosphere-ionosphere coupling currents in Jupiter's middle magnetosphere: Effect of precipitation-induced enhancement of the ionospheric Pedersen conductivity, *Ann. Geophys.*, *22*(5).
Nichols, J. D., and S. W. H. Cowley (2005), Magnetosphere-ionosphere coupling currents in Jupiter's middle magnetosphere: Effect of magnetosphere-ionosphere decoupling by field-aligned auroral voltages, *Ann. Geophys.*, *23*(3), 799–808.
Nichols, J. D., J. T. Clarke, J. C. Gérard, D. Grodent, and K. C. Hansen (2009), Variation of different components of Jupiter's auroral emission, *J. Geophys. Res.*, *114*, A06210, doi:10.1029/2009JA014051.
Nichols, J. D., N. Achilleos, and S. W. Cowley (2015), A model of force balance in Jupiter's magnetodisc including hot plasma pressure anisotropy, *J. Geophys. Res. Space Physics*, *120*, 10,185–10,206, doi:10.1002/2015JA021807.
Nichols, J. D., et al. (2017), Response of Jupiter's auroras to conditions in the interplanetary medium as measured by the Hubble Space Telescope and Juno, *Geophys. Res. Lett.*, doi:10.1002/2017GL073029, in press.
Paranicas, C., et al. (2017), Radiation near Jupiter detected by Juno/JEDI during PJ1 and PJ3, *Geophys. Res. Lett.*, *44*, 4426–4431, doi:10.1002/2017GL072600.
Ray, L. C., Y. J. Su, R. E. Ergun, P. A. Delamere, and F. Bagenal (2009), Current-voltage relation of a centrifugally confined plasma, *J. Geophys. Res.*, *114*, A04214, doi:10.1029/2008JA013969.
Ray, L. C., R. E. Ergun, P. A. Delamere, and F. Bagenal (2010), Magnetosphere-ionosphere coupling at Jupiter: Effect of field-aligned potentials on angular momentum transport, *J. Geophys. Res.*, *115*, A09211, doi:10.1029/2010JA015423.
Ray, L. C., R. E. Ergun, P. A. Delamere, and F. Bagenal (2012), Magnetosphere-ionosphere coupling at Jupiter: A parameter space study, *J. Geophys. Res.*, *117*, A01205, doi:10.1029/2011JA016899.
Ray, L. C., N. A. Achilleos, M. F. Vogt, and J. N. Yates (2014), Local time variations in Jupiter's magnetosphere-ionosphere coupling system, *J. Geophys. Res. Space Physics*, *119*, 4740–4751, doi:10.1002/2014JA019941.
Saur, J., Pouquet, A. and Matthaeus, W. H. (2003), An acceleration mechanism for the generation of the main auroral oval on Jupiter. *Geophys. Res. Lett. 30*(5), 1260, doi:10.1029/2002GL015761.
Scudder, J. D., E. C. Sittler Jr., and H. S. Bridge (1981), A survey of the plasma electron environment of Jupiter: A view from Voyager, *J. Geophys. Res.*, *86*, 8157–8179.
Sharp, R. D., E. G. Shelley, and G. Rostoker (1975), A relationship between synchronous altitude electron fluxes and the auroral electrojet, *J. Geophys. Res.*, *80*, 2319–2324, doi:10.1029/JA080i016p02319.
Sittler, E. C., and D. F. Strobel (1987), Io plasma torus electrons—Voyager 1, *J. Geophys. Res.*, *92*, 5741–5762, doi:10.1029/JA092iA06p05741.
Su, Y.-J., R. E. Ergun, F. Bagenal and P. A. Delamere (2003), Io-related Jovian auroral arcs: Modeling parallel electric fields, *J. Geophys. Res. 108*(A2), 1094, doi:10.1029/2002JA009247.
Valek, P. W., et al. (2017), Hot flow anomaly observed at Jupiter's bow shock, *Geophys. Res. Lett.*, doi:10.1002/2017GL073175, in press.
Vogt, M. F., M. G. Kivelson, K. K. Khurana, R. J. Walker, B. Bonfond, D. Grodent, and A. Radioti (2011), Improved mapping of Jupiter's auroral features to magnetospheric sources, *J. Geophys. Res.*, *116*, A03220, doi:10.1029/2010JA016148.
Vogt, M. F., E. J. Bunce, M. G. Kivelson, K. K. Khurana, R. J. Walker, A. Radioti, B. Bonfond, and D. Grodent (2015), Magnetosphere-ionosphere mapping at Jupiter: Quantifying the effects of using different internal field models, *J. Geophys. Res. Space Physics*, *120*, 2584–2599, doi:10.1002/2014JA020729.